Contents lists available at ScienceDirect

Animal Behaviour

Identifying cues for self-organized nest wall-building behaviour in the rock ant, *Temnothorax rugatulus*, using hidden Markov models

E. Invernizzi [a, *] , T. Michelot [b] , V. Popov [b] , N. Ng [a] , E. Macqueen [a] , A. Rouviere [a] ,
M. Webster [a] , T. Sasaki [c]

[a] *Centre for Biological Diversity, University of St Andrews, U.K.*
[b] *Centre for Research into Ecological and Environmental Modelling, University of St Andrews, U.K.*
[c] *Odum School of Ecology, University of Georgia, Athens, GA, U.S.A.*

ARTICLE INFO

European *Temnothorax albipennis* and its American counterpart *Temnothorax rugatulus* build circular walls to limit their nest area within a rock crevice. To determine wall position, workers are thought to rely on a distance template (from the cluster of brood and nurses at the nest centre) and on indirect social (i.e. stigmergic) information found in the aggregations of already-deposited building material. Analytical and simulation models of this behaviour predict that the combination of these two mechanisms can produce the observed wall structure, but there is so far no empirical evidence of either mechanism. Here, we find statistical evidence in support of the stigmergic relationship between stone density and deposition behaviour. We apply hidden Markov models (HMMs) to analyse wall-building data from four colonies of *T. rugatulus*. We show that material deposition activity changes following a parabolic relationship with the density of building material at building sites, different from the linear relationship hypothesized previously. This parabolic curve is similar to behavioural response curves identified in the nest enlargement process of several ant species. In addition, HMM analysis indicates the existence of two distinct states in *T. rugatulus* building activity. These states are associated with different mean building rates (that is, the two states can be described as a high and a low activity state) and might be caused by changes in task priorities during the colony process of settling into a new nest. This study updates one of the earliest models of self-organized animal behaviour.

An Early Model of Self-Organized Animal Behaviour

In the late 1980s and early 1990s, the study of self-organization in physical and biological systems witnessed its first burst of computational and experimental activity, not least due to the advances in computational power that introduced spatial simulations as a methodology in scientific research (Camazine et al., 2001; Kauffman, 1993). One of the earliest models in the field of collective animal behaviour reconstructed nest wall building in *Temnothorax* ants as the result of a simple, collectively applied and coherent rule set (Franks & Deneubourg, 1997; Franks et al., 1992). This model has been included in a textbook well known in the subfield of self-organization in biology (Camazine et al., 2001), which collects

studies investigating the underlying mechanisms of collective patterns across a variety of biological systems; thus, this case study of *Temnothorax* ants is one of the staple introductory examples for researchers new to this area of biology. However, at least to our knowledge, this behavioural model has never been empirically tested. In this paper, we apply statistical analysis to *Temnothorax* wall-building data to investigate the cue—response relationship proposed by the model, specifically the role of local stone density in guiding deposition behaviour.

Nest Wall Building in Temnothorax Ants

Many ant species of the genus *Temnothorax* form small colonies that inhabit confined areas, such as acorn cavities or rock crevices. Due to the fragility of their nest sites, they frequently migrate to a

* Corresponding author.
 E-mail address: edith.invernizzi@outlook.com (E. Invernizzi).

new nest (Möglich, 1978). At least two species in this large genus, *Temnothorax albipennis* and *Temnothorax rugatulus*, are known to build a circular wall that delimits and protects the new nest site; typically, the wall is constructed by stone deposition rather than by excavation. The resulting wall structure is one of the simplest structures produced by eusocial insects, but its construction is still not fully understood. Our case study offers an exceptional opportunity to investigate social insect nest building under laboratory conditions.

The current behavioural model of *Temnothorax* nest wall building (Franks & Deneubourg, 1997; Franks et al., 1992) hypothesizes that stone deposition and pick-up activity are guided by two rules: a template-based rule determining building distance from the centre of the nest and a positive feedback effect (generated by the density of the stones already present at building sites) modulating building rates. While this model seems to capture the key mathematical dynamics of the building process (as shown in spatial simulations; Chapter 17 in Camazine et al., 2001; Franks & Deneubourg, 1997; Franks et al., 1992), there are a few shortcomings.

First, there is so far no experimental or statistical evidence indicating what cues guide the behaviour: the model is based on observational data (Franks et al., 1992) supported by computational simulations (Camazine et al., 2001; Franks & Deneubourg, 1997; Franks et al., 1992). Namely, the model proposes that *Temnothorax* workers use the cluster of brood and nurse ants (positioned at the centre of the nest) as a reference point for a distance template. Building rate in the model is also supposed to be modulated by stone density. The focal mechanism is thought to be as follows: a worker's propensity for stone deposition increases as it physically comes across other stones, so that, the larger a stone pile, the more likely the pile is to attract further depositions. Conversely, isolated stones or small heaps are more likely to be picked up and moved to a larger pile. These two dynamics, corresponding (respectively) to positive and negative feedback, would ensure that building activity is co-localized at the most active building site, which is likely to be near the (possibly optimal) distance defined by the template rule. The modulation of building activity through cues that are themselves generated by the building process (stigmergy; Grassé, 1939) is a known feedback mechanism in eusocial insect collective nest building (Buhl et al., 2005; Fouquet et al., 2014; Khuong et al., 2016; Rasse & Deneubourg, 2001; Toffin et al., 2009).

A second noticeable issue with previous studies is that they were based on data extracted during the initial phase of the behaviour, when the wall is far from complete (Franks & Deneubourg, 1997; Franks et al., 1992). While the current behavioural model satisfactorily reproduces the shape of the wall observed in nature when applied to wall building beyond the initial phase (i.e. until it generates a complete wall), recent work (Invernizzi & Ruxton, 2021) has shown that there are two limitations: (1) the model leads to the formation of an incomplete wall when building material is limited and (2) it lacks a termination mechanism that brings wall expansion to an end. With regard to the first limitation, limited material availability in the simulation leads to the behavioural algorithm producing clumps of material, rather than a wall (even a partial one). In nature (or in the laboratory), the wall-building performance of *Temnothorax* colonies in conditions of low material availability has not (to our knowledge) been tested. Consequently, the prediction of poor performance obtained from the simulations leaves us facing two alternative considerations: either the behavioural model is correct, and these species fail to build a complete wall when material is scarce, or the model is incomplete, and further work is needed. We believe that the second hypothesis is more likely. The second limitation (the lack of a behavioural termination mechanism in the model) is based

on the finding that, in computational simulations, the wall keeps expanding in thickness as long as there is material available, because deposition rate never decreases once it has reached its maximum. Given that the cost, to the colony, in time and energy of such behaviour makes this an unrealistic feature in a natural process, we believe that this second limitation also calls for an extension to the current model.

In this article, we present an extension that solves the second shortcoming (introducing a termination mechanism) and partially addresses the first (finding statistical evidence supporting the use of stone density as a behavioural cue). We first tested this change with a computational simulation and then proceeded to find evidence for it in empirical data. Before we introduce our extended model, however, we need to describe two features of ant colony activity that determined our choice of analysis.

The Problem with Ant Colonies

A key problem, when analysing ant activity data sets, is accounting for colony states. By 'state', we mean a change in the overall activity patterns of the workers, which, in turn, affects the level of activity measured in single tasks (e.g. foraging, building, brood care, etc.). An example of such change in patterns would be a switch in colony priorities from foraging to closing gaps in the nest walls in response to rain: high engagement in foraging shifts towards high engagement in building. There are two processes in ant colonies that may induce changes in colony state and thus increase or decrease the measured activity rate value. The first one, which we have just mentioned in our example, is interaction between tasks. It is known that perturbations to one task, such as worker removal, decrease the number of workers in other tasks in some ant species. This is because workers are reallocated from other tasks to the one that has become high demand (*Pogonomyrmex barbatus*: Gordon, 1986, 1987, 1989; *Pogonomyrmex badius*: Kwapich & Tschinkel, 2013, 2016). *Temnothorax rugatulus* and *T. albipennis* workers exhibit weak specialization but high segregation: that is, they perform more than one task but are consistently found associated with wider task groups (Charbonneau & Dornhaus, 2015b). For example, *T. rugatulus* builders are also foragers but not brood workers. These workers are likely to switch to other tasks if demand increases, decreasing the activity levels for the previous task even if other conditions are unchanged (Gordon, 1986, 1987).

The second state change-inducing process is the occurrence of periodic shifts in activity levels that is typical of some ant species (Cole & Trampus, 1999). We know that many species (of which the most studied is *Leptothorax allardycei*; Cole, 1991a, 1991c, 1992; Cole & Hoeg, 1996; Franks et al., 1990) display oscillations in the total activity of their colonies, from phases during which the majority of workers is active to phases in which the majority is inactive. This periodicity is unrelated to circadian rhythms and indeed occurs on much shorter timescales (tens of minutes). Measurements of colony activity, accordingly, are affected by the overall colony activity state. This phenomenon begins at the individual level. Workers display chaotic behavioural switches between an active state, during which they are engaged in a task or walking around the nest (Leitner & Dornhaus, 2019), and an inactive one, throughout which they remain immobile (Cole, 1991a, 1991c). The reason behind these shifts is unclear: some models assume chaotic locomotory activity generated by the underlying neural network (Miramontes et al., 2001), while others model ant activity as a function of the energy levels of the colony, in relation to food storage and digestion (Hemerik et al., 1990). Both models can reproduce the observed patterns. In colonies, these individual worker phases become synchronized through the physical interaction of workers (Cole, 1991a, 1991b; Cole &

Trampus, 1999; Franks et al., 1990) and the colony acquires an activity pattern with a periodic component. Does *T. rugatulus* display periodic activity? A recent study has shown that it indeed does, albeit the degree of periodicity varies among colonies (Doering et al., 2019).

Switches between colony states are expected to cause changes in measured building rates even when building-specific behavioural cues remain unchanged. The task-specific behavioural model can thus be better understood by accounting for state switches as a separate phenomenon. This can be done by using the right statistical approach. Specifically, state changes can be incorporated in a statistical model by assuming that a time series contains observations drawn from two separate distributions, each associated with a colony level state (e.g. specialized workers engaged in building versus foraging; or occurrence of active versus inactive phase). The process of switching between states can be modelled as a Markov chain even if the exact sequence of states is unknown (hidden). Hidden Markov models (HMM), which are well established in ecology, offer a statistical framework to carry out inference on unobserved Markov chains (McClintock et al., 2020). They also account for temporal autocorrelation in the measurements and the effects of covariates can be included in the distribution of observations in each state, analogously to linear modelling. Importantly, applying this approach does not require being able to identify which underlying process is causing the changes in state: the process remains unknown. We used this framework to infer the relationship between predictors and deposition rate in our time series.

Aims of the Study

In the present study, we had three aims. First, we sought statistical support for a feedback effect of stone density at building sites in the nest wall-building behavioural model of *Temnothorax*. This feedback effect is consistent with the existing behavioural model proposed by Franks et al. (1992) but has not been empirically tested. Second, we wished to extend the original behavioural model to incorporate termination of building activity. We hypothesized that negative feedback is crucial for decreasing, and eventually terminating, the deposition activity. Third, we hypothesized that stone density is the cue guiding termination, by exercising a negative effect on activity after a certain density at building sites has been reached. This is a parsimonious hypothesis, because it implies that worker activity is modulated by one cue only (stone density) throughout the duration of building.

We first performed a spatial computational simulation, in which we tested the ability of the extended model to produce a complete wall similar to that observed in nature. We then empirically tested the existence of a stone density-dependent feedback effect of building sites on worker building activity rates, using laboratory data of *T. rugatulus*. We compared two model types, which we fitted using hidden Markov models: (1) a positive feedback-only model (i.e. modelling a positive correlation between stone density and stone deposition rate; model 1) representing the model proposed by Franks et al. (1992), Franks and Deneubourg (1997) and Camazine et al. (2001); (2) a positive + negative feedback model (i.e. modelling a change in the relationship between stone density and stone deposition rate, from positive to negative, depending on the stone density value; model 2), representing our extended model. The first model can be approximated, mathematically and statistically, by a linear model, while the second model can be represented by a quadratic model. We additionally tested for the effect of distance from the brood cluster (i.e. the template component of the behavioural model) in each model type (models 3 and 4).

METHODS

Agent-Based Model

The architecture of the agent-based model is identical to the one applied in Invernizzi and Ruxton (2021), which is itself a replication of the original model found in Camazine et al. (2001). The behavioural model of nest wall building that we used assumes that workers rely on two pieces of information for picking up and depositing a pellet: the distance from the brood and nurse cluster, which acts as a template, and the number of stones surrounding the location. The only difference between the simulations reported here and those reported in Invernizzi and Ruxton (2021) is found in the equation (described below) that models the relationship between probability of deposition (D_x) and stone density at each deposition location x. For convenience, we summarize the characteristics of the agent-based model below.

The simulations consist in the movement of agents (the workers) in two-dimensional space. The space is represented by a matrix of 81×81 point locations (hence referred to as nodes), where locations with adjacent coordinates are considered to be adjacent in space. The space contains 1000 building blocks (the pellets), which are randomly and uniformly scattered across space at the beginning of the simulation. Agents encountering pellets may pick one up and may deposit it at the next encountered location, with probability dependent on the pick-up function P_x (defined as $P_x = P(X = x)$) and on the deposition function D_x (defined as $D_x = D(X = x)$), respectively. The pick-up probability is defined as:

$$P_x = P_M \left(1 - \frac{1}{1 + \tau(r - r_o)^2} \right) \times F(S). \qquad (1)$$

Here, r is the distance of location x from the centre of the brood cluster, r_o is an optimal distance value known to all workers at which the wall should be built, S is the total number of stones nearby, summed to include the current node x and the neighbouring four nodes (north, south, west and east of x), P_M is the maximum possible probability of deposition if we ignore the effect of the stones and $F(S)$ is the effect of the stones:

$$F(S) = \begin{cases} F_M & \text{for } S < S_c \\ F_m & \text{for } S \geq S_c \end{cases} \qquad (2)$$

where S_c is a critical number of stones after which the behaviour changes, and with $F_m < F_M$.

The deposition probability is defined as

$$D_x = D_M \frac{1}{1 + \tau(r - r_o)^2} \left(G_m + (G_M - G_m) \times e^{-\frac{(S_x - S_c)^2}{2}} \right). \qquad (3)$$

The first part of the right-hand side of this equation (outside the brackets) is similar to equation (1), representing the effect of distance from the brood cluster on the maximum possible value of deposition probability (not accounting for the effect of stones), D_M. The second part of the right-hand side, within the brackets, represents the effect of the number of stones on deposition probability as a bell curve: the effect reaches its maximum value, G_M, if the number of stones at the current location, S_x, equals the critical number of stones, S_c. Away from this quantity, the value of the effect of number of stones decreases with the difference between S_x and S_c following a normal curve, plateauing at its minimum value G_m. Therefore, overall, the curve of D_x at a single location x changes, following the shape of a bell curve, according to the number of stones at that location x.

Note that this equation differs from the equation in the original model (Camazine et al., 2001):

$$D_x = D_M \frac{1}{1 + \tau(r - r_O)^2} G(S)Q \qquad (4)$$

where $Q = 0$ if the maximum stone carrying capacity at that node has already been reached and $Q = 1$ otherwise. The effect of stones on deposition in this equation is

$$\begin{cases} G(S) = G_M \text{ if } S \geq S_c \\ G(S) = G_m \text{ if } S < S_c \\ \qquad G_m < G_M. \end{cases} \qquad (5)$$

In this original equation, a change in the local number of stones S of one unit causes a jump in the upper bound of the deposition probability from $D_M \times G_m$ to $D_M \times G_M$, without intermediate values. In our model, in contrast, the effect grows proportionally with the value of S. Biologically, we can think of this as a proportional increase in the resistance that a laden ant encounters when dragging its stone across a stone pile; the larger the stone pile (the bigger S), the higher the probability that the ant will drop the stone it is carrying.

At each round of the simulation, the following events occur. (1) The first agent moves to a random location in the matrix, chosen with uniform probability. (2) If there is at least one pellet present at the location, the agent picks it up with probability P_x. (3) If the agent has picked up a pellet, it moves to a new, randomly and uniformly chosen location. (4) If the current number of pellets at the new location is below the carrying capacity of the node, the agent deposits its pellet with probability D_x. Steps 3–4 are repeated until the pellet is deposited. (5) Steps 1–4 are repeated for all agents.

Each simulation contains 30 agents and is run for 5000 rounds. Longer simulations (up to 20 000 rounds) were tested and showed that the emerging wall structure reached an equilibrium point by the 1000th round; that is, the location and density of the wall did not change after this point.

The parameter values used in the simulations are identical to the original model. They are $P_M = 0.35$, $D_M = 0.5$, $G_M = F_M = 0.55$, $G_m = F_m = 0.01$, $S_c = 6$, $\tau = 0.025$ and $r_O = 18$. The maximum carrying capacity of a node is six stones.

Colonies

Four colonies of *T. rugatulus* were used for the experiments (for details on colony origin and keeping, see Ethical Note). The main limited factor of sample size was the extent of manual data collection and processing involved in this study. Colonies were collected from the wild (Pinal Mountains near Globe, AZ, U.S.A.; N 33°19.00′N, 110°52.56′W) during the summer of 2019. After collection, colonies were kept in a temperature-controlled laboratory room at the University of Georgia (Atlanta, GA, U.S.A.) and subject to 12:12 h dark:light cycles. Temperature was set to 13 °C during dark hours and 22 °C during light hours. Individual colonies were housed in 12×12 cm plastic boxes, pierced to ensure airflow. For nesting, they were given an artificial cavity made of two 75×50 mm microscope slides separated by cardboard corners of size $100 \times 100 \times 1.15$ mm (Franks et al., 1992). The top slide was opaque. In nature, this species nests in rock crevices with minimal natural light access and this set-up adequately reproduces the natural environment. Each box included a water tube and a tray of agar-based diet that were refreshed (Bhatkar & Whitcomb, 1970). After the experiment, the colony was placed back in the housing box together with the new nest cavity.

Colony sizes and approximate numbers of brood items are reported in Table 1. All colonies used were monogynous with no alates present. Each colony was used once.

Experimental Procedure

Experiments were conducted during the summer of collection, over the course of 2 months. Each colony was tested on a separate day. Experiments were run in a light-optimized set-up (see Filming Set-up) and filmed, starting from the moment the colony was introduced in the new environment. Experiments took place in an arena box where the workers were free to move and where the new nest and the stones could be easily found (Fig. 1). The arena consisted in a $20 \times 27.5 \times 9.75$ cm open plastic box with Fluon-coated walls that prevented escape from the arena. A clean, empty artificial cavity consisting of two 75×50 mm microscope slides separated by cardboard corners (Franks et al., 1992) was provided as a potential nest site in the arena. The top slide was opaque to mimic the darker nesting environments typical of these species. Before the start of the experiment, a pile of 4 g of black 0.4–0.6 mm aquarium gravel (of a similar size to the sand described in Franks et al., 1992, where the authors report an average grain size of 0.5 mm) was placed in front of the new nest, approximately 4 cm away from the side of the artificial cavity facing the arena. The arena, as well as the stones and the slides used to build the new nest, was cleaned with 90% ethanol the day before every experiment. No food or water was provided during the experiment.

Experiments started in the early morning, between 0630 and 0830 hours. Immediately after the start of the recording, the colony was removed from the housing box and the original nest opened by cutting the tape that held the slides together. The bottom slide (where the queen, brood and majority of workers are found) was placed in the arena and the remaining ants were gently brushed off from the top slide or removed from the housing box with a pair of tweezers. The colony was then left to spontaneously migrate to the new nest, where the new wall would be built. Filming continued for a total of 39 h.

Filming Set-up

Video recordings of building behaviour were taken in a set-up optimized to guarantee uniform light conditions (Fig. 1). Three lights (right, left and rear) were placed adjacent to a white diffuser containing the arena. Filming was done with a Sony FDR-AX100E camera placed approximately 30 cm above the arena floor. Camera height was controlled for in the data by converting pixels to millimetres using the microscope slide as a reference. The videos were shot at 25 frames/s in 4K resolution. The original video files are available upon request. Modified video files showing only the areas of observations (see Fig. 1c) are publicly available in the Open Science Framework (Foster & Deardorff, 2017) online depository (https://osf.io/xvbgf/).

Table 1
Size and approximate number of brood items in each colony

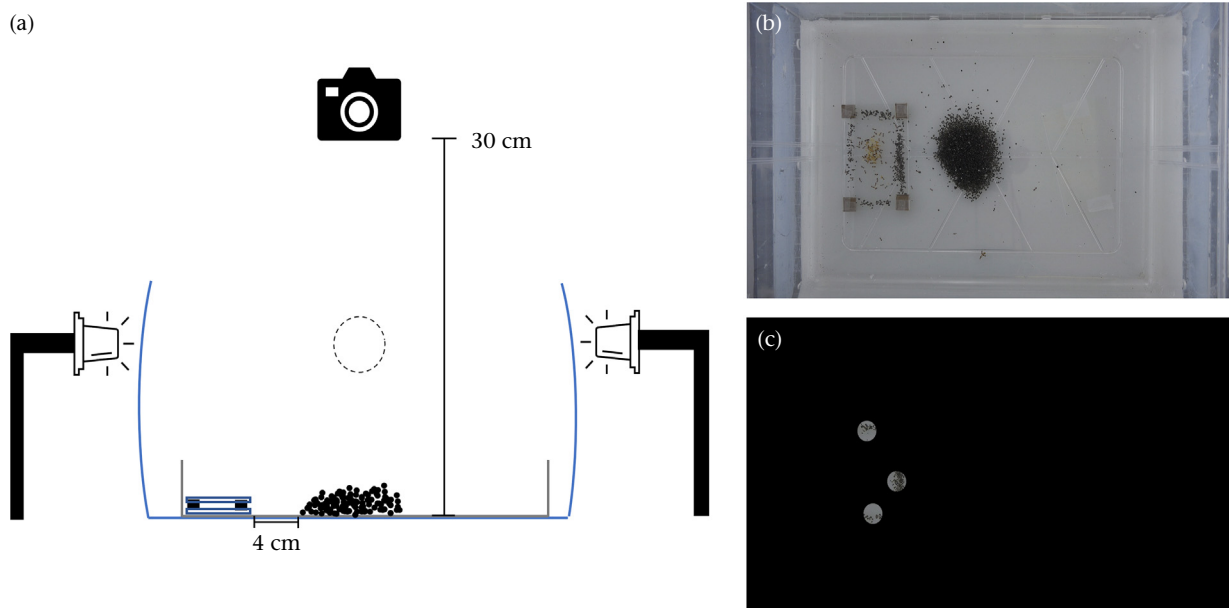| Colony (video file)	Workers	Brood items (approximate)
Colony 1 (R05)	68	15
Colony 2 (R29)	89	20
Colony 3 (R34)	108	15
Colony 4 (R54)	120	30

Figure 1. Experimental set-up and image processing for data collection. (a) Simplified drawing of the set-up as seen from the front. The blue lines represent the sides of the white diffuser fixture and the black lines represent the building arena. The artificial cavity was placed against either the left wall or the back wall of the arena, with building stones piled approximately 4 cm from it. The dotted circle represents the third (back) light. (b) Video frame extracted from one of the colony videos. (c) The same frame in (b) after a digital black mask was applied to the file, so that only the three selected building sites were visible to the observer for behavioural event recording.

Data Collection

Out of the total video length, we used the first few hours of building activity for continuous observation (i.e. observations from the same colony come from a single, continuous observation time block), totalling an average of 9 h per colony (7.5−11.5 h depending on colony). The criterion used to choose the end point of the observation period is described below.

Observation Sites

Using the final video frame of each colony's recordings, we selected three distinct building sites corresponding to sections of the final wall as observation areas. The sites were chosen haphazardly, but purposely on three different sides of the wall, to control for any biases in ant preferred building side. The choice of using three sites was motivated by the consideration that this number is large enough to account for variance among building sites, but small enough to ensure sufficient distance between them (i.e. the sites can be considered independent in the sense that any effect of predictors can be attributed to the predictor value at that site, rather than at a nearby site; the predictor's effect on worker behaviour is assumed to be localized). At each chosen site, we measured the final wall width and extracted its midpoint co-ordinates using FIJI software (see Software for version details). All colony videos were then blackened out, leaving only three 75-pixel radii (i.e. 6.35−6.60 mm, depending on the colony; this was due to small differences in the height of the camera) areas, centred on the extracted coordinates. These isolated areas (building sites) were used as independent areas of observations to collect building data (Fig. 1c).

Start and End of the Observation Period

Our criterion for determining the duration of data collection was as follows. For all colonies, behavioural recording started at the start of the experiment and the start of building activity was defined as the first deposition event (see below for the definition of deposition used) at any of the three building sites. To determine the end point of behavioural recording, we first collected observations until each site had reached 49 stones (i.e. at least 0.36 stones/mm). This high number of stones means that stones are too packed together for the observer to be able to accurately count them. Because building proceeds with independent speed at each site, this approach resulted in time series of varying length. We then extended the two shorter time series in each colony to match the length of the longest time series, so as to obtain, for each colony, three time series covering the same time period. The number of stones at each site in these extended time series (i.e. after manual count could no longer be performed) was tracked by adding deposition events to the stone count and subtracting pick-up events from the stone count.

Behavioural Event Coding

Only two types of behavioural events are most germane for building activity and both were accordingly recorded in our data collection: stone deposition and stone pick-up. Stone deposition was defined as the positioning of a carried stone by an ant at any location within the building site. This could happen by lifting (the worker lifts the stone over the ground during transport, using its mandibles), by bulldozing (as described by Franks et al., 1992: the worker pushes the stone in front of itself on the ground) or by dragging (the ant pulls the stone through the nest using its mandibles while moving backwards towards the chosen deposition site). Lifting and dragging are the most common stone-moving behaviours in *T. rugatulus*, in contrast to the use of bulldozing by *T. albipennis* reported by Franks et al. (1992). This might be due to the larger size of *T. rugatulus* workers, which enables them to lift stones of similar weight whereas *T. albipennis* have to push them. Accordingly, dragging was observed most often with larger stones. Stone pick-up was defined as the removal of a previously deposited stone either (1) for deposition at a location greater than one ant length (approximately) away within the same building site, or (2) for carrying out of the site (presumably

for deposition at a different location; the worker was out of sight when it left the circular area). Note that pick-up events of type (1) also counted as a deposition event.

Variables

For each observed event, we recorded the time of occurrence and the number of stones in the site at the time of the event (the latter of which was used to calculate stone density). The number of stones was counted manually. The event rate was calculated by counting events over 15 min intervals, starting from the first deposition event in the colony. The per-minute rate, calculated as the number of events/15 min, was used in the analysis. Pick-up rate was also calculated, but, due to the low frequency of pick-up events and to the limited sample size, the statistical model could not be reliably fit. That is because, if the sample size is small and the events are rare, then there is little information in the data about the model parameters, and the estimation procedure is susceptible to numerical instability (i.e. the optimizer might fail to identify sensical parameter values). Therefore, model fitting was limited to deposition rate. We used pick-up rate only to evaluate whether colony activity showed a similar pattern of shifts in activity levels across nest-building activities.

We measured the distance between the brood cluster and each building site from frame shots taken at 15 min intervals from the start of building activity (i.e. these time points overlap with the end of the interval over which the per-minute rate was calculated). To measure this variable, we first had to define what constitutes the brood cluster. We defined ants as belonging to the brood cluster if they were within 1.5 ant lengths of a brood item (egg, larva, pupa or queen) or of another ant belonging to the cluster. We then manually drew the contours of this area, following the profile of the ants that were part of it, using FIJI software, and extracted the coordinates of the area's centroid (in pixels). We calculated the distance between the brood cluster and the building site as the Euclidean distance between the cluster centroid and the centre of the site.

All measurements taken in pixels (i.e. distance and building site area) were converted to millimetres. The pixel-to-millimetre ratio was obtained for each video using the known length of a side of the microscope slide as reference.

Hidden Markov Models

Methodology

It is reasonable to assume that ants undergo different, unobservable behaviour states, each of them associated with a different building activity, measured by the deposition rate. A suitable statistical modelling tool in this context are hidden Markov models (HMMs). HMMs (McClintock & Michelot, 2018; Rabiner, 1989) are an established method in animal movement ecology. They assume the existence of an unobserved (hidden) process, which switches between a finite number of states through time, each associated with a different probability distribution for the observed variable(s). In our scenario, the hidden process is assumed to represent the overall colony level sequence of behavioural states, which can roughly be interpreted as low and high rates of building activity.

There are two main components to estimate in an HMM: (1) transition probabilities between the states; (2) state-dependent parameters of the observation distributions (Fig. 2a). From a fitted HMM, it is also possible to predict the most likely state sequence given the data (Fig. 2b), as it is often of great interest to infer which observations were generated by each state. The HMM methodology has been extended so that it is possible to specify any of the parameters as functions of covariates, using an approach similar to generalized linear models.

HMMs have been used, for example, to identify different behavioural states, such as foraging and resting, from movement data, and to estimate the effect of covariates such as group status, season and environment on movement parameters or on behavioural transition probabilities (McKellar et al., 2015; van Beest et al., 2019). In our study, we have assumed the existence of two hidden colony states, corresponding to whether building activity is prioritized (high activity state) or workers are instead mostly engaged in other tasks or inactive (low activity state).

HMM fitting and model comparison

We assumed that the deposition rate followed a gamma distribution in each state, parametrized in terms of mean and standard deviation. The choice of gamma distribution was made based on the observable skew in the frequency distribution of rate values (see Results). A problem associated with the choice of the Gamma distribution is that it is defined for positive values, while we had several observations taking the value 0. To work around this problem for each such observation we drew a uniformly distributed random variable taking a value between 0 and the minimum observed deposition rate.

Data from each colony and site were treated as independent time series. We assumed that model parameters are the same between and within colonies (between building sites) because they are generated by the same underlying building behavioural model. The only model parameter assumed to be colony-specific is the intercept, which captures colony-specific activity features (e.g. a colony might have more workers specialized in building compared to another). In this model, each site within a colony is driven by its own hidden state sequence, to allow for local variations in activity levels (due, for example, to delays in period syncing across the colony, or to variations in numbers of workers active at any one building site that might appear in the data as differences in activity state). The Viterbi algorithm (Viterbi, 2006) was used to estimate the most likely state sequence.

In each fitted HMM model, a different relationship between mean deposition rate and predictors was assumed to have generated the data. The full list of models is found in Table 2. We fitted the models using a numerical optimization of the likelihood function (McClintock & Michelot, 2018). This procedure is sensitive to the starting parameter values given to the optimizer. Therefore, we fitted each model 200 times with different (randomly generated) sets of starting values searching for the global maximum of the likelihood function. Because of the high number of trials used, we believe that the estimated parameters are close to those of the global optimum. The goodness-of-fit analysis (see the paragraph below), as well as the comparison of the observations simulated from the model with the real data (see Results), provide further evidence for the adequacy of the model fit.

The goodness-of-fit was evaluated using the pseudo-residuals of the fitted HMMs (analogous to linear model residuals). All fitted models passed the residual check (i.e. the pseudo-residuals appeared normally distributed and their autocorrelation coefficient was close to zero) and were included in an information criterion-based comparison, using Akaike's method (Akaike's Information Criterion or AIC; Akaike, 1974). We then used posterior predictive checking on the best model: that is, we compared patterns between the observed time series and simulations from the model, to check that important features were captured.

Software

The agent-based model was built in Python 3.6 (Van Rossum & Drake, 2009). For video data analysis, individual building sites were
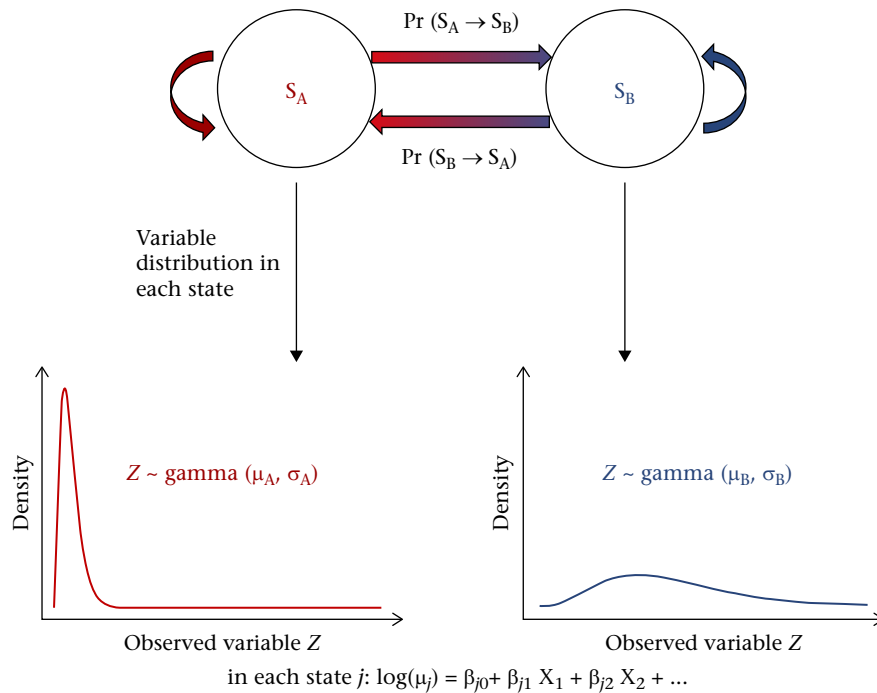
Figure 2. Schematic representation of hidden Markov model (HMM) estimation. Simplified representation of the HMM formulation. The two model components are (1) a set of hidden states (here, S_A and S_B) with associated transition probabilities and (2) a probability distribution for the data variable (Z) within each state, described by some state-specific parameters (here, the mean μ_j and standard deviation σ_j). The state-dependent mean parameter is influenced by predictors (x) through a generalized linear model.

isolated from the rest of the video using FFmpeg software (version N-94383-g3883c9d147; Bellard & FFmpeg Team, 2000) and the opencv (Bradski, 2000) and numpy (Oliphant, 2006) libraries for Python 3.6 (Van Rossum & Drake, 2009). Measurements (i.e. brood cluster centroid) from video frames were taken using FIJI (Schneider et al., 2012). Data processing and statistical analysis were conducted in R, version 4.3.1, using the hmmTMB package (Michelot, 2022).

Ethical Note

The data were collected under the University of Georgia's ethics guideline on animal handling and welfare. Ants are not covered by the Animal Scientific Procedures Act (ASPA) guidelines. The experiments required the colonies to perform nest migration following disruption of the old nest. This type of event poses temporary stress to the colony but is not believed to have long-term effects on its wellbeing or survival. After the end of our study, colonies were kept for use in other experiments.

RESULTS

This study wants to extend the existing behavioural model of *Temnothorax* wall building by incorporating and testing two hypotheses: (1) *Temnothorax* ants use the density of stone deposited at building sites as a feedback cue guiding construction; (2) stone density modulates the rate of building activity from start to termination. Our study was theory driven: to test whether a behavioural model incorporating both hypotheses leads to the formation of wall structures similar to the ones built in nature, we first used an agent-based model. Once the theoretical results were known, we sought empirical evidence by conducting a statistical analysis of deposition activity in *T. rugatulus* colonies, comparing models with different predictors and shape of the relationship between stone density and response (Table 2).

Agent-Based Model Predictions

The computational simulations confirm that the extended behavioural model produces a wall structure similar to the one built by *T. albipennis* and *T. rugatulus* under laboratory conditions. Fig. 3 shows a sample output of the agent-based model, under conditions of limited stone availability (1000 stones; Fig. 3a) and of intermediate stone availability (3000 stones; Fig. 3b). Iterating the simulation 100 times shows that, having set a distance template that optimizes deposition at 18 mm distance from the brood cluster, stones are consistently deposited within close proximity to this value ('1000 stones' condition: the mean distance is 18.18 cm, with a standard deviation of 0.15 cm; the minimum mean distance across simulations is 17.86 cm and the maximum 18.72 cm. '3000 stones' condition: the mean distance is 18.76 cm, with a standard deviation of 0.18 cm; the minimum mean distance across simulations is 18.36 cm and the maximum 19.20 cm). This performance is qualitatively similar to that of the Franks and Deneubourg model at intermediate stone availability; however, the Franks and Deneubourg model performs poorly when building material is scarce, resulting in a wall with many gaps. To assess the degree to which deposition in the extended model occurs uniformly in a circular shape (i.e. with no gaps), we can use the measure of circular dispersal called circular spread or $\bar{R}$:

$$\bar{R} = \frac{1}{M} \sqrt[2]{\sum_{i=1}^{M} \cos \theta_i^2 + \sum_{i=1}^{M} \sin \theta_i^2} \qquad (6)$$

with M being the total number of deposition locations and θ_i the angle of each location i measured in radians. Note that $\bar{R}$ is thus a value comprised between 0 and 1, where 0 indicates perfect uniformity in circular dispersal (deposition occurs equally at all angles around the circle).

Table 2
Fitted models

Model	μ_D
Model 1	$\mu_D = \exp (\text{stone density} + \text{c})$
Model 2	$\mu_D = \exp (\text{stone density} + \text{stone density}^2 + \text{c})$
Model 3	$\mu_D = \exp (\text{stone density} + \text{distance} + \text{c})$
Model 4	$\mu_D = \exp (\text{stone density} + \text{stone density}^2 + \text{distance} + \text{c})$

List of all statistical models fitted to the state-dependent hidden Markov model (HMM) parameters. The data points in each state are said to be drawn from a gamma distribution, defined by the mean of deposition rate D, μ_D, and by its standard deviation SD_D. Only the mean is assumed to depend on covariates. Models were formulated based on the parameters thought to guide deposition behaviour, from existing literature (see main text). The constant c is the intercept.

Over 1000 iterations, we find that the circular dispersal of deposited stones is highly uniform, with a mean of 0.09 and a standard deviation of 0.05 in simulations run with 1000 stones (minimum value of 0.009 and maximum value of 0.25), and a mean of 0.03 and a standard deviation of 0.02 in simulations run with 3000 stones (minimum value of 0.002 and maximum value of 0.08). The extended model is therefore an improvement on the original model in terms of how reliably a good-quality wall is built across environments (Fig. 3c). To quantify the effect of the underlying behavioural model on the value of circular spread, we ran the simulations with both models (all other conditions being equal)

and then fitted a linear regression model on the circular spread values obtained. We used circular spread as the dependent variable and stone availability and model type as predictors (this approach is equivalent to running a t test, but it avoids the issues that come with applying this type of statistics to simulated data; White et al., 2014). With this approach, we detect that model type has an effect size of 0.05, that is, nests generated from the extended behavioural model have, on average, a circular spread value that is 0.05 units lower than nests generated from the original model. To put this into perspective, if we look at the quantiles of all circular spread values, we can see that the core 50% (i.e. the values comprised but not included between the bottom 25% and the top 25%) sits between a value of 0.03 and a value of 0.12. The effect size of switching to the extended model is over half of the distance between these two boundaries. We can also compare the quantiles of the circular spread values obtained from the extended model (0%: 0.00; 25%: 0.02; 50%: 0.05; 75%: 0.09; 100%: 0.25) with the quantiles from the original model (0%: 0.01; 25%: 0.06; 50%: 0.10; 75%: 0.14; 100%: 0.37) to get an idea of how much the two distributions differ.

To understand whether these results can be generalized to other parameter values, we conducted a sensitivity analysis of the agent-based model and found that results are highly robust (see Appendix). This is important because it means that we expect these results to be consistent no matter what parameters might be estimated empirically.
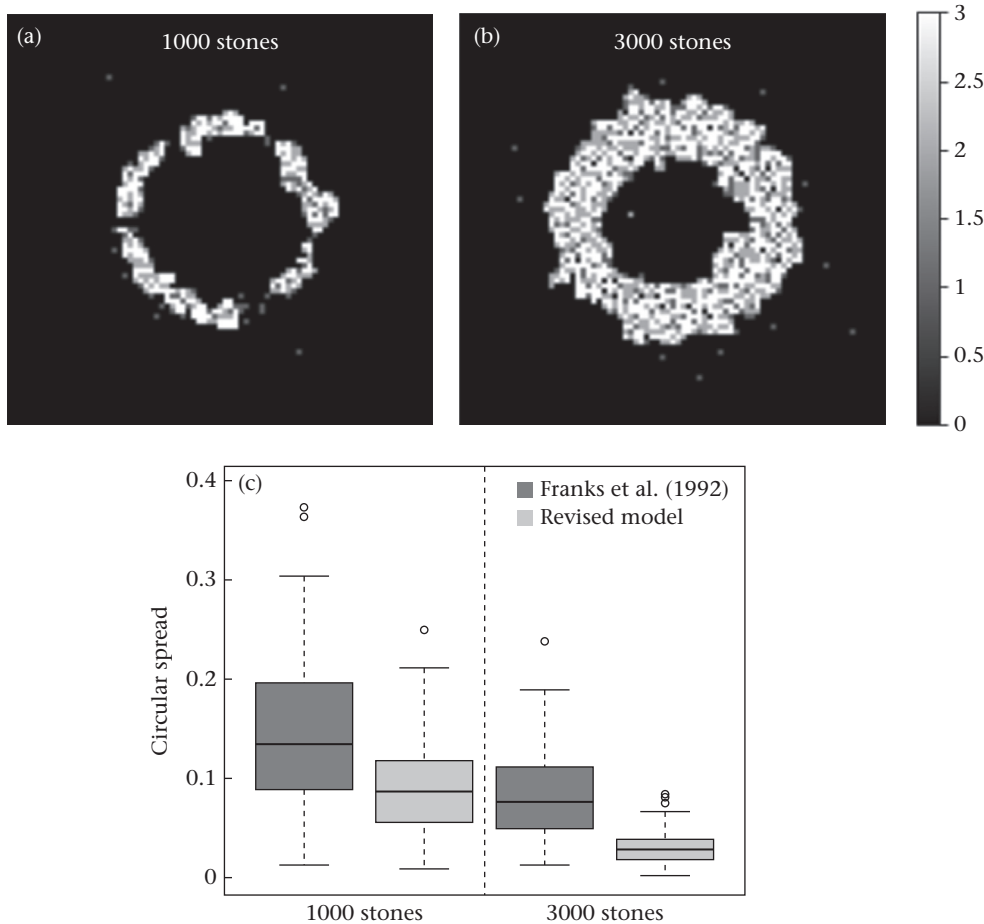

Figure 3. Two example outputs of the agent-based model incorporating the double feedback effect of neighbouring stone density on deposition activity at a building site. (a) Output under limited building material (stone) availability, which produces a circular but incomplete wall. (b) Output of the same simulation run when the number of stones available in the simulation is increased to 3000, which leads to the formation of a full wall. The greyscale shows the number of stones at each location. (c) Box plot of circular dispersal values across simulation runs in the original model (Franks et al., 1992) and in our revised version. The revised model resulted in a substantial increase in the evenness of the distribution of building material across the ideal circumference (i.e. the wall had fewer gaps).

Experimental Data Analysis

The statistical analysis of laboratory data supports the existence of two alternating colony behavioural states affecting building activity rates. In both states, the best statistical model assumes that stone density at building sites is positively correlated with deposition rate at low values and negatively correlated with deposition rate at high values (see below).

Building activity showed alternating periods of slow rate increase with periods of slow decrease (Appendix, Fig. A2). Deposition and pick-up activity had similar rates at the same time points (Fig. 4), suggesting changes in the overall activity of the colony.

We reiterate here our proposed explanations for these patterns (already detailed in the Introduction), for which we identified two possible, nonmutually exclusive causes. First, *T. rugatulus* displays high segregation in worker task groups and partial specialization within tasks and workers that take care of nest building and repair are also foragers (Charbonneau & Dornhaus, 2015a). Alternatively, or additionally, *T. rugatulus* colonies may undergo periodic activity shifts between high and low activity phases. The trend that we observe does not show regular oscillations, but there might be a hidden periodic component that only becomes evident when the appropriate mathematical analysis is applied. A previous study has shown that *T. rugatulus* displays periodic oscillations in activity (Doering et al., 2019). In addition, we note that the activity pattern observed does not appear to be affected by the time of day (Appendix, Fig. A3).

Based on the observed patterns, and independently from the cause behind activity shifts, we built our statistical models assuming that the time sequence of rates is the product of two combined distributions: one corresponding to the phase of high building activity and one to the phase of low activity. The building behaviour underlying each of the two distributions is assumed to

Table 3
Model selection

Model	One-state HMM	Two-state HMM
Model 1	−116.6049	−177.3058
Model 2	−134.6801	**−190.9976**
Model 3	124.8332	−173.9603
Model 4	−139.6240	−187.6706

Comparison of models using Akaike's information criterion. The one-state HMM is a classical GLM with gamma-distributed dependent variable. The value in bold is the lowest AIC form the eight models.

be generated by the same process (a worker rule set encoding response to environmental cues; i.e. a behavioural model) but to reflect a quantitative change in individual behaviour that is caused by colony state: the distributions differ in their mean and standard deviation. The sequence of states, which determines the distribution from which each observation in a time series arises, can be inferred from a fitted hidden Markov model.

In Table 2, we list the relationship between the mean of the distributions and the predictors analysed for each behavioural model. Note that each behavioural model corresponds to a distinct statistical model. In Table 3, we show the Akaike's information criterion (AIC; Akaike, 1974) value of each fitted model.

For each model formulation, we fitted a one-state HMM, i.e. a standard generalized linear model (GLM) with gamma-distributed dependent variable (deposition rate) and log link function. For each model specification, a two-state HMM was preferred over the GLM, indicating that there is some evidence that the dynamics of the deposition process are driven by different states. Among the four candidate formulations, with different covariates included on the mean deposition rate, the model favoured by AIC was a two-state HMM with a quadratic relationship of stone density. The model
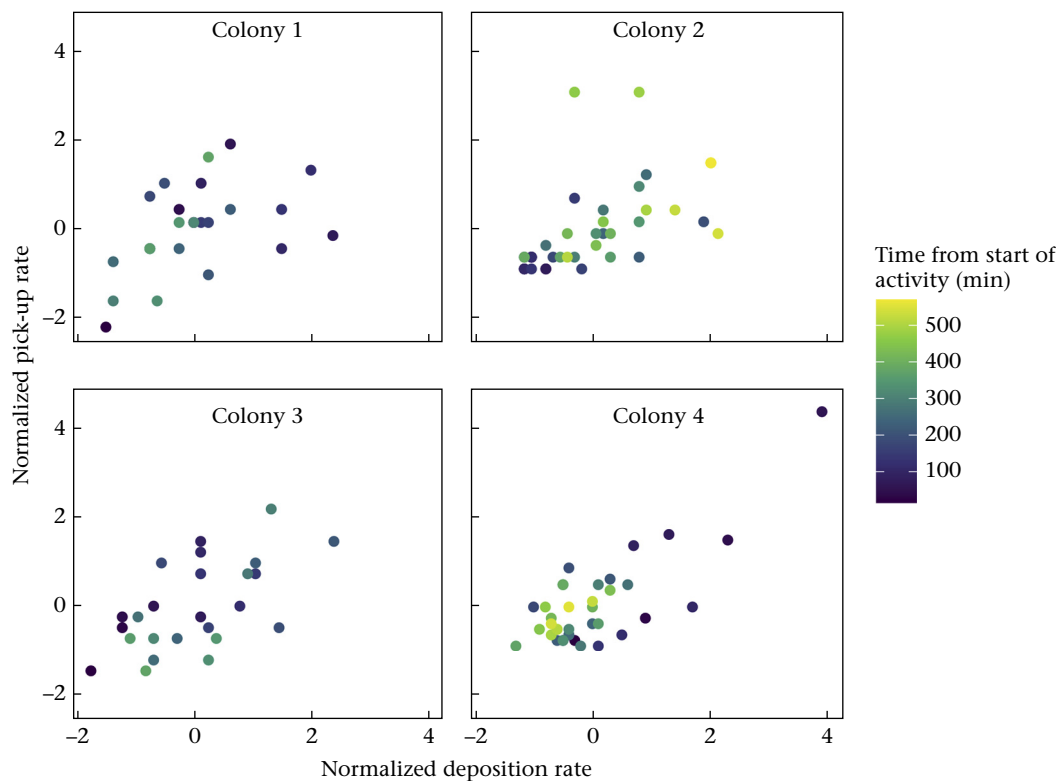

Figure 4. Relationship between rates of different building activities across building time. Building activity rates of each colony were normalized by their mean value and plotted against each other. Colour scale shows the time point (min) from the start of building activity to the end of data collection. Rates were calculated as the total number of events across the three colony sites, divided by the time interval (events/min). Observations began with the start of building, defined as the first deposition event in the colony, and ended when at least 60 stones had been deposited at all three building sites under observation. Each rate value was calculated over a 15 min interval.

with distance as an additional covariate only had a marginally higher (worse) AIC, but that model suffered from more numerical instability due to the greater number of estimated parameters, so we decided to work with the simpler model.

Fig. 5 shows the transition parameters of the hidden Markov chain generating the state sequence and the estimated state distributions assuming mean predictor values. The estimated deposition probability distributions seem to support the interpretation of the two states: state 1 tended to capture periods of lower activity and state 2 tended to capture periods of higher activity (Fig. 5b). This interpretation is also consistent with the state sequence estimated for each colony, shown in the Appendix, Fig. A4.

Table 4 shows the effect sizes of the best model and Fig. 6 displays the relationship between the stone density covariate and the mean value of deposition rate. For any value of the stone density and for all four colonies, the estimated mean deposition rate is always higher in state 2 than in state 1 (Fig. 6).

DISCUSSION

Summary of Results

In this study, we have used an HMM approach to distinguish between building activity measurements taken during periods when this task is prioritized and periods where workers are either inactive or engaged in other tasks. Building activity does therefore not occur at a constant pace up to wall completion, but rather depends on other colony level factors. We also show that stone density found at building sites has a two-fold role as a behavioural cue: it increases nearby deposition activity at low and intermediate value and it decreases deposition (relative to the peak rate) at high values. This latter effect is a new finding that constitutes an extension to the original behavioural model (Franks & Deneubourg, 1997; Franks et al., 1992).

We wish to discuss two limitations of our analysis here. First, our sample size was relatively small (four colonies) given the complexity of the statistical models used. Sample size does not affect state sequence inference, which occurs at the level of the single observation in HMMs. It can lead to large uncertainty in covariate effects, but in our case the confidence intervals of the relationship between stone density and deposition activity were narrow and the AIC comparison supported a quadratic rather than a linear relationship between covariates. Small sample size also negatively affects the stability of estimated parameters (that is, convergence of the likelihood cannot be achieved). While this problem means that we can provide no guarantee that the best model fit we have identified is a global rather than local maximum, yet, given the high number of trials used in the fitting process, we
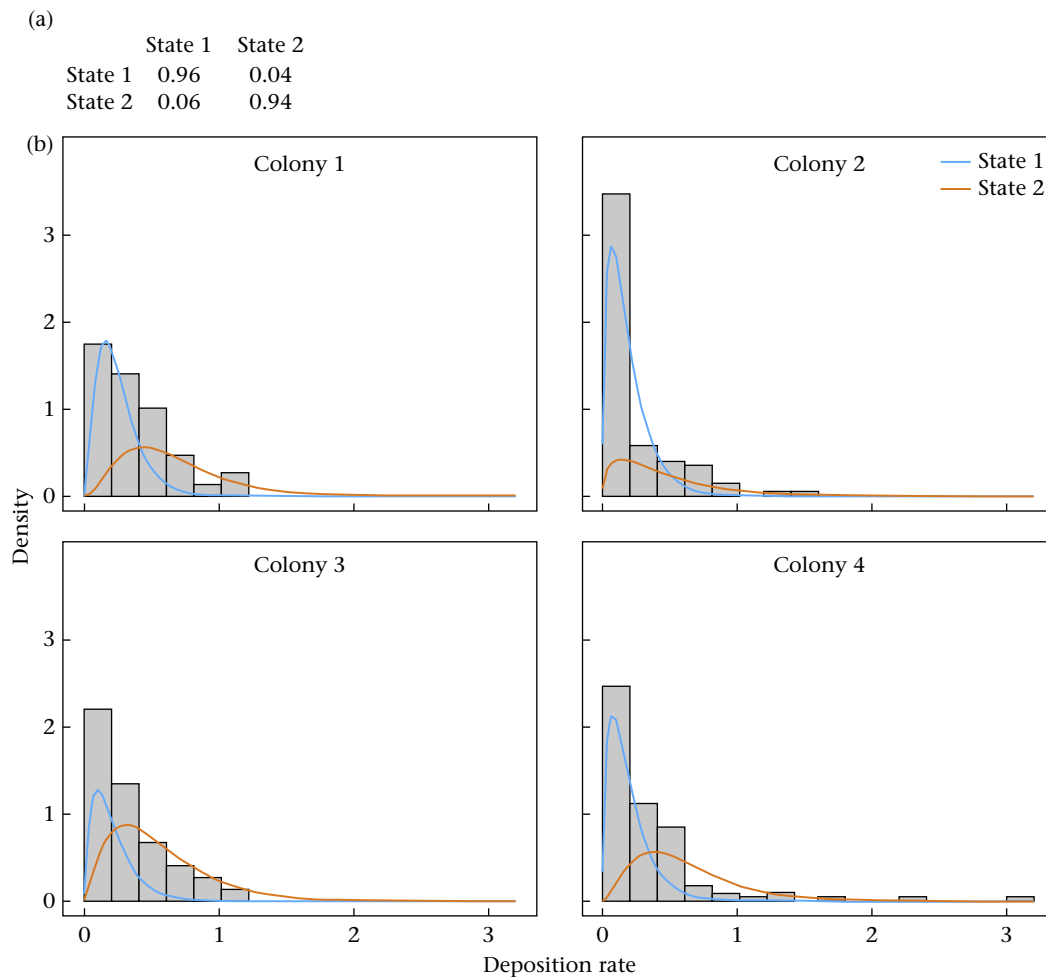

Figure 5. Hidden Markov chain parameters and observation distributions of each colony as estimated from model 2. (a) Transition probabilities between states; that is, the probability of a colony being in each state at time point t given its state at time point $t − 1$. (b) Estimated gamma distribution of deposition rate associated with each activity state (state 1, state 2) against the density histogram of the observed distribution, for each colony. Distribution plots were generated from the model parameters shown in Table 4, with the assumption that the covariate was fixed to the mean observed stone density in the whole data set.

Table 4
Fitted parameters of model 2

	Intercept (Colony 1)		Covariate effect				
	Mean	SD	Stone density	(Stone density)^2	Colony 2	Colony 3	Colony 4
State 1	−1.764	−1.895	2.051	−2.776	−0.279	−0.187	−0.256
State 2	−0.662	−1.000	1.040	−1.046	−0.373	−0.157	−0.062

Model parameter values by state.

believe that the estimated parameters are close to if not identical with those of the global maximum and the uncertainty around these estimates is captured by the provided confidence intervals. Second, the shifts in activity levels measured in our analysis might be caused by changes in the energy level of workers. We did not provide food during our experiments, but colonies were moved to the arena directly from the housing box, where food was available ad libitum, and the activity data analysed correspond to the first 10 h of the experiment only. Starvation has been shown to increase forager activity, but only after several days (Franks et al., 1990); consequently, we believe that our colonies were unlikely to be affected. Some species of ants preferentially perform certain activities depending on time of day (Gordon, 1983), but building activity in *T. rugatulus* does not seem to be one such case.

In our Introduction to this article, we discussed ant activity states as colony level phenomena, in which the whole worker population synchronizes into either a high or a low activity state. Our results show that the three building sites that we tracked within each colony were most commonly found in different states (Appendix, Fig. A4). This could mean that the two states picked up by our analysis correspond to shifts in task priority within the colony, rather than periodic changes in overall colony activity rates. There are, however, other explanations. Activity state synchronization at the colony level is achieved through worker physical interactions (Cole, 1991c). *Temnothorax rugatulus* colonies are small (Table 1) and only a subset of the workers engages in building. It is possible that interactions at the edge of the colony (where building occurs) are rarer and synchronization is often only achieved at a local level, between neighbouring sites (Cole and colleagues showed that borderline periodicity starts with a group size of 5–7 workers in *L. allardycei*). However, because only a few workers build, some periods of low activity detected at a site may simply be periods during which no worker was active at that specific site (perhaps being instead active at a neighbouring site just outside our observation area). Future studies that look at building activity across a larger number of sites and perhaps measure activity levels for other tasks, with individual worker tracking, will be able to tell us which one among these explanations is correct.

Stone Density as a Behavioural Cue

In the past two decades, the application of advanced techniques (such as x-ray tomography) to the study of nest structures has led to remarkable developments in the field (Perna & Theraulaz, 2017), giving us data that had previously been hard or even impossible to obtain. *Temnothorax* nests are simple structures, but these types of tools can add considerable value, allowing us, for example, to observe the internal structure of a nest without disrupting its
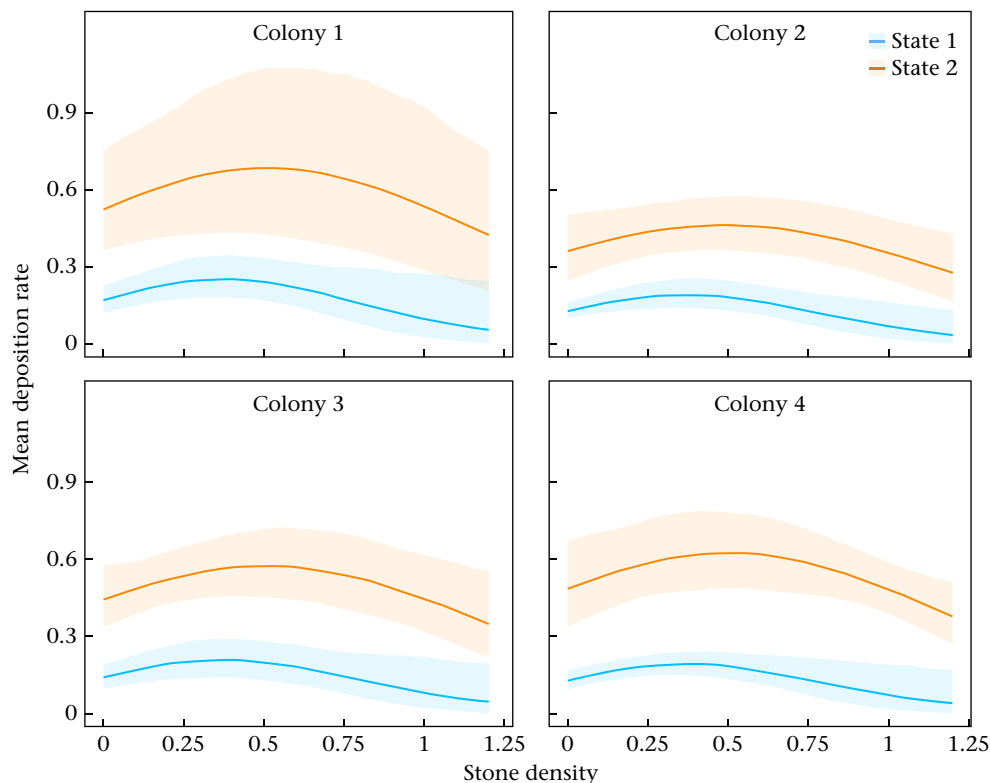

Figure 6. Relationship between stone density and mean deposition rate in each colony for each state in model 2. Shaded areas show the 95% confidence interval.

external structure (Varoudis et al., 2018). Below, we discuss what insights on building behaviour we can draw from our study and how the application of advanced tools, or simply future studies, can help elucidate some aspects that are still open to interpretation.

The observed response of workers to stone density is a case of stigmergic feedback. Stigmergy is a well-known concept in social insect building and can be defined as the effects that changes in the architecture created by past building activity have on current worker building behaviour. This phenomenon has been discovered in several eusocial insect species (Ireland & Garnier, 2018; Khuong et al., 2016; Perna & Theraulaz, 2017). For example, in the Formosan subterranean termite, workers use depressions in the ground, including those left by other excavating workers, as stigmergic cues promoting further excavation (Bardunias & Su, 2009). The use of stone density is a case of material density, in particular, being used as a stigmergic cue, which is not uncommon (Buhl et al., 2005; Fouquet et al., 2014; Khuong et al., 2016).

Does the relationship between stone density and deposition rate that we detected unequivocally point to this cue as the direct modulator of the behaviour (i.e. what the worker perceives and responds to)? Certainly not so. *Temnothorax rugatulus* workers might be responding to stone density directly (i.e. through quantitative or qualitative evaluation of stone pile conformation), or indirectly, through changes in an environmental cue that is affected by stone deposition. For example, the intensity of air currents and the amount of light penetrating the nest from the sides are alternative factors whose change is foreseeably correlated to changes in stone density. Air currents, in particular, have been shown to modulate ant behaviour in a similar deposition and pick-up context: that of corpse disposal (Jost et al., 2007). Recent studies (Khuong et al., 2016; Petersen et al., 2015), moreover, indicate that pheromones are sometimes used by termites as a cue modulating building or general labour, and similar mechanisms might be important in ants. We would like to stress, however, that close observations of laden ants who carry a stone by dragging shows that they seemingly pull their load against the pre-existing heap, stopping when the stone encounters a lot of resistance. Thus, at least when dragging, *T. rugatulus* builders appear to actively use stone density to guide their activity, through mechanical contact. Similarly, Franks et al. (1992) reported that *T. albipennis* workers bulldoze the stone they are carrying into existing piles. Both species, therefore, appear to be using contact with stone piles for building, even if in slightly differing ways.

Experimental manipulation is necessary to determine what cues the ants respond to in this case of nest building. Close observation or manipulation of individual ant behaviour, for example, might shed some light on what cues the worker responds to, while the observation of building behaviour in more natural environments, such as acorns or crevices, will also grant us more information on how other potential cues, beside stone density, change during building.

One Cue to Modulate Them All

The identified quadratic relationship between stone density and deposition rate meets the hypothesis that nest size regulation depends on a local amplification—long-range inhibition (LALI) process driven by building sites and their stigmergic role. This is similar to the mechanism underlying nest excavation in other ant species (Buhl et al., 2005; Halley et al., 2005; Rasse & Deneubourg, 2001). In some species (*Messor sancta*, *Linepithema humile* and *Lasius niger*), the coupling of a positive and a negative feedback effect is achieved through the use of one cue, building site density. Site density increases with the ratio between colony and nest size, because stochastic initiation-of-excavation events become clustered in time

and space, triggering a positive feedback loop. Once the nest has sufficiently expanded, this ratio decreases, eventually leading to behavioural termination through lack of sufficient cues. When a wall is first built by *T. albipennis* or *T. rugatulus*, the template component of the building algorithm (if it exists) limits nest expansion. The negative feedback effect is caused, as we have seen, by a direct or indirect response to stone density. Only in the additional case of nest enlargement after an increase in colony size (or before a prospective increase in colony size), removal and relocation of stones from the old wall might be triggered by the template shifting outwards (here, the hypothesis of a single cue being used breaks down), as cluster size increases, while the same mechanism guiding termination during initial wall building also leads to termination here.

Is the existence of a LALI mechanism guiding nest size regulation in many ant species a case of convergence or of common origin? When considering common origin, we must remind ourselves of the fact that *Temnothorax* are capable of nest excavation, beside the occupation of empty cavities coupled with wall building. The process of excavation in these species has not yet been studied. Should it be discovered that it shares common rules with the species already listed, it is possible that the LALI mechanism found in wall building derives from this shared mechanism, through step-by-step change (e.g. the switch to air currents as a cue, the emergence of a template).

Conclusion

Our results confirm that stone density at building sites is involved in a feedback loop with deposition activity and is sufficient, as a cue, for both increasing building activity rates and inducing building termination later in the process. We have shown here that HMMs are an effective statistical approach for separating the data into phases associated with different colony level states, thus accounting for fluctuations in worker activity. The use of HMMs can help address similar questions in other colony tasks, as well as in other eusocial systems, thus enhancing our understanding of division of labour and task organization. If incorporated into mathematical and simulation models, these studies can also help address ecological and evolutionary questions on the ecological properties and evolution of self-organized behaviour in eusocial species.

Author Contributions

Contributions are listed in order of magnitude of work contributed. Concept: E.I. and T.S. Agent-based model: E.I. Data collection: experiments and video processing by E.I.; video analysis by R.A., M.E., E.I. and N.N. Statistics: V.P., T.M., E.I. Figures: E.I., T.M. and N.N. Revisions: T.M., V.P. and E.I. equally.

Data Availability

All data and code files used for this study can be found here: https://github.com/invernie/Hidden-Markov-models-of-Temnothorax-nest-building. Video files modified so that only the areas of observation are visible are found in the Open Science Framework online depository (https://osf.io/xvbgf/). The original video files are too large to be included in online databases and are available upon request by contacting the corresponding author.

Declaration of Interest

We declare no conflict of interest.

Acknowledgments

We are grateful to Dr Kazutaka Soji (University of Tokyo) and to Ben Taylor, M.Sc. (University of Georgia Athens), for their help with filming set-up and video processing. We also thank the referees for their contributions to improving the original manuscript and in particular for proposing new useful ways to visualize the data. E.I.'s Ph.D. was funded by the John Templeton Foundation as part of the research collaboration grant 'Putting the extended evolutionary synthesis to the test' (grant no. 60501). The postdoctoral research project that followed this initial work was funded by an ASAB research grant to M.W. and E.I.

References

Akaike, H. (1974). A new look at the statistical model identification. *IEEE Transactions on Automatic Control, 19*, 716−723.

Bardunias, P., & Su, N. Y. (2009). Opposing headings of excavating and depositing termites facilitate branch formation in the Formosan subterranean termite. *Animal Behaviour, 78*(3), 755−759. https://doi.org/10.1016/j.anbehav.2009.06.024

Bellard, F., & FFmpeg Team. (2000). *FFmpeg (Version N-94383-g3883c9d147)*. https://ffmpeg.org.

Bhatkar, A., & Whitcomb, W. H. (1970). Artificial diet for rearing various species of ants. *Florida Entomologist, 53*(4), 229−232. https://doi.org/10.2307/3493193

Bradski, G. (2000). The OpenCV library. *Dr. Dobb's Journal of Software Tools, 120*, 122−125.

Buhl, J., Deneubourg, J.-L., Grimal, A., & Theraulaz, G. (2005). Self-organized digging activity in ant colonies. *Behavioral Ecology and Sociobiology, 58*(1), 9−17. https://doi.org/10.1007/S00265-004-0906-2

Camazine, S., Deneubourg, J.-L., Franks, N. R., Sneyd, J., Theraulaz, G., & Bonabeau, E. (2001). *Self-organization in biological systems*. Princeton University Press.

Cariboni, J., Gatelli, D., Liska, R., & Saltelli, A. (2007). The role of sensitivity analysis in ecological modelling. *Ecological Modelling, 203*(1−2), 167−182. https://doi.org/10.1016/j.ecolmodel.2005.10.045

Charbonneau, D., & Dornhaus, A. (2015a). Workers 'specialized' on inactivity: Behavioral consistency of inactive workers and their role in task allocation. *Behavioral Ecology and Sociobiology, 69*(9), 1459−1472. https://doi.org/10.1007/s00265-015-1958-1

Charbonneau, D., & Dornhaus, A. (2015b). When doing nothing is something. How task allocation strategies compromise between flexibility, efficiency, and inactive agents. *Journal of Bioeconomics, 17*(3), 217−242. https://doi.org/10.1007/s10818-015-9205-4

Cole, B. J. (1991a). Is animal behaviour chaotic? Evidence from the activity of ants. *Proceedings of the Royal Society B: Biological Sciences, 244*(1311), 253−259. https://www.jstor.org/stable/76608.

Cole, B. J. (1991b). Short-term activity cycles in ants: A phase−response curve and phase resetting in worker activity. *Journal of Insect Behavior, 4*, 129−137.

Cole, B. J. (1991c). Short-term activity cycles in ants: Generation of periodicity by worker interaction. *American Naturalist, 137*(2), 244−259. https://doi.org/10.1086/285156

Cole, B. J. (1992). Short-term activity cycles in ants: Age-related changes in tempo and colony synchrony. *Behavioral Ecology and Sociobiology, 31*, 181−187.

Cole, B. J., & Hoeg, L. (1996). The influence of brood type on activity cycles in Leptothorax allardycei (Hymenoptera: Faruicidae). *Journal of Insect Behavior, 9*(4), 539−547. https://doi.org/10.1007/BF02213878

Cole, B. J., & Trampus, F. I. (1999). Activity cycles in ant colonies: Worker interactions and decentralised control. In C. Detrain, J. L. Deneubourg, & J. M. Pasteels (Eds.), *Information processing in social insects* (pp. 289−307). Springer. https://doi.org/10.1007/978-3-0348-8739-7.

Doering, G. N., Sheehy, K. A., Lichtenstein, J. L. L., Drawert, B., Petzold, L. R., & Pruitt, J. N. (2019). Sources of intraspecific variation in the collective tempo and synchrony of ant societies. *Behavioral Ecology, 30*(6), 1682−1690. https://doi.org/10.1093/BEHECO/ARZ135

Foster, E. D., & Deardorff, A. (2017). Open science framework (OSF). *Journal of the Medical Library Association, 105*(2). https://doi.org/10.5195/JMLA.2017.88. Article 203.

Fouquet, D., Costa-Leonardo, A. M., Fournier, R., Blanco, S., & Jost, C. (2014). Coordination of construction behavior in the termite Procornitermes araujoi: Structure is a stronger stimulus than volatile marking. *Insectes Sociaux, 61*(3), 253−264. https://doi.org/10.1007/S00040-014-0350-X

Franks, N. R., Bryant, S., & Griffiths, R. (1990). Synchronization of the behaviour within nests of the ant Leptothorax acervorum (fabricius)−I. Discovering the phenomenon and its relation to the level of starvation. *Bulletin of Mathematical Biology, 52*(5), 597−609. https://doi.org/10.1016/S0092-8240(05)80368-4

Franks, N. R., & Deneubourg, J.-L. (1997). Self-organizing nest construction in ants: Individual worker behaviour and the nest's dynamics. *Animal Behaviour, 54*(4), 779−796. https://doi.org/10.1006/anbe.1996.0496

Franks, N. R., Wilby, A., Silverman, B. W., & Tofts, C. (1992). Self-organizing nest construction in ants: Sophisticated building by blind bulldozing. *Animal Behaviour, 44*(2), 357−375. https://doi.org/10.1016/0003-3472(92)90041-7

Gordon, D. M. (1983). The relation of recruitment rate to activity rhythms in the harvester ant, *Pogonomyrmex barbatus* (F. Smith) (Hymenoptera: Formicidae). *Journal of the Kansas Entomological Society, 56*(3), 277−285. https://www.jstor.org/stable/25084411.

Gordon, D. M. (1986). The dynamics of the daily round of the harvester ant colony (Pogonomyrmex barbatus). *Animal Behaviour, 34*, 1402−1419.

Gordon, D. M. (1987). Group-level dynamics in harvester ants: Young colonies and the role of patrolling. *Animal Behaviour, 35*, 833−843.

Gordon, D. M. (1989). Dynamics of task switching in harvester ants. *Animal Behaviour, 38*, 194−204.

Grassé, P.-P. (1939). La reconstruction du nid et le travail collectif chez les termites supérieurs. *Journal de Psychologie Normale et Pathologique, 30*, 370−396.

Halley, J. D., Burd, M., & Wells, P. (2005). Excavation and architecture of Argentine ant nests. *Insectes Sociaux, 52*, 350−356. https://doi.org/10.1007/s00040-005-0818-9

Hemerik, L., Britton, N., & Franks, N. R. (1990). Synchronization of the behaviour within nests of the ant *Leptothorax acervorum* (fabricius)—II. Modelling the phenomenon and predictions from the model. *Bulletin of Mathematical Biology, 52*(5), 613−628. https://doi.org/10.1016/s0092-8240(05)80369-6

Invernizzi, E. (2022). *Building models: Developing the behavioural model of Temnothorax collective wall building to study the evolutionary robustness of self-organised algorithms*. Ph.D. thesis. University of St Andrews. https://doi.org/10.17630/STA/374.

Invernizzi, E., & Ruxton, G. D. (2021). Updating a textbook model of collective behavior: Nest wall building in *Temnothorax albipennis*. *Animal Behavior and Cognition, 8*(2), 231−239. https://doi.org/10.26451/abc.08.02.09.2021

Ireland, T., & Garnier, S. (2018). Architecture, space and information in constructions built by humans and social insects: A conceptual review. *Philosophical Transactions of the Royal Society B: Biological Sciences, 373*(1753), 26−35. https://doi.org/10.1098/rstb.2017.0244

Jost, C., Verret, J., Casellas, E., Gautrais, J., Challet, M., Lluc, J., Blanco, S., Clifton, M. J., & Theraulaz, G. (2007). The interplay between a self-organized process and an environmental template: Corpse clustering under the influence of air currents in ants. *Journal of the Royal Society Interface, 4*(12), 107−116. https://doi.org/10.1098/rsif.2006.0156

Kauffman, S. A. (1993). *The origins of order*. Oxford University Press.

Khuong, A., Perna, A., Sbaï, C., Combe, M., Kuntz, P., Jost, C., & Theraulaz, G. (2016). Stigmergic construction and topochemical information shape ant nest architecture. *Proceedings of the National Academy of Sciences of the United States of America, 113*(5), 1303−1308. https://doi.org/10.1073/pnas.1509829113

Kwapich, C. L., & Tschinkel, W. R. (2013). Demography, demand, death, and the seasonal allocation of labor in the Florida harvester ant (*Pogonomyrmex badius*). *Behavioral Ecology and Sociobiology, 67*(12), 2011−2027. https://doi.org/10.1007/s00265-013-161

Kwapich, C. L., & Tschinkel, W. R. (2016). Limited flexibility and unusual longevity shape forager allocation in the Florida harvester ant (*Pogonomyrmex badius*). *Behavioral Ecology and Sociobiology, 70*(2), 221−235. https://doi.org/10.1007/s00265-015-2039-1

Leitner, N., & Dornhaus, A. (2019). Dynamic task allocation: How and why do social insect workers take on new tasks? *Animal Behaviour, 158*, 47−63. https://doi.org/10.1016/j.anbehav.2019.09.021

Möglich, M. (1978). Social organization of nest emigration in *Leptothorax* (Hym., Form.). *Insectes Sociaux, 25*(3), 205−225. https://doi.org/10.1007/BF02224742

McClintock, B. T., Langrock, R., Gimenez, O., Cam, E., Borchers, D. L., Glennie, R., & Patterson, T. A. (2020). Uncovering ecological state dynamics with hidden Markov models. *Ecology Letters, 23*(12), 1878−1903. https://doi.org/10.1111/ELE.13610

McClintock, B. T., & Michelot, T. (2018). momentuHMM: R package for generalized hidden Markov models of animal movement. *Methods in Ecology and Evolution, 9*(6), 1518−1530. https://doi.org/10.1111/2041-210X.12995

McKellar, A. E., Langrock, R., Walters, J. R., & Kesler, D. C. (2015). Using mixed hidden Markov models to examine behavioral states in a cooperatively breeding bird. *Behavioral Ecology, 26*(1), 148−157. https://doi.org/10.1093/beheco/aru171

Michelot, T. (2022). *hmmTMB: Hidden Markov models with flexible covariate effects in R*. https://arxiv.org/abs/2211.14139v2.

Miramontes, O., Solé, R. V., & Goodwin, B. C. (2001). Neural networks as sources of chaotic motor activity in ants and how complexity develops at the social scale. *International Journal of Bifurcation and Chaos, 11*(6), 1655−1664. https://doi.org/10.1142/S0218127401002912

Oliphant, T. E. (2006). *A guide to NumPy*. Trelgol.

Perna, A., & Theraulaz, G. (2017). When social behaviour is moulded in clay: On growth and form of social insect nests. *Journal of Experimental Biology, 220*(1), 83−91. https://doi.org/10.1242/jeb.143347

Petersen, K., Bardunias, P., Napp, N., Werfel, J., Nagpal, R., & Turner, J. S. (2015). Arrestant property of recently manipulated soil on *Macrotermes michaelseni* as determined through visual tracking and automatic labeling of individual termite behaviors. *Behavioural Processes, 116*, 8−11. https://doi.org/10.1016/j.beproc.2015.04.004

Rabiner, L. R. (1989). A tutorial on hidden Markov models and selected applications in speech recognition. *Proceedings of the IEEE, 77*(2), 257−286. https://doi.org/10.1109/5.18626

Rasse, P., & Deneubourg, J.-L. (2001). Dynamics of nest excavation and nest size regulation of *Lasius niger* (Hymenoptera: Formicidae). *Journal of Insect Behavior, 14*(4), 433−449. https://doi.org/10.1023/A:1011163804217

Saltelli, A. (2002). Making best use of model evaluations to compute sensitivity indices. *Computer Physics Communications, 145*(2), 280−297. https://doi.org/10.1016/S0010-4655(02)00280-1

Saltelli, A., Annoni, P., Azzini, I., Campolongo, F., Ratto, M., & Tarantola, S. (2010). Variance based sensitivity analysis of model output. Design and estimator for the total sensitivity index. *Computer Physics Communications, 181*(2), 259−270. https://doi.org/10.1016/j.cpc.2009.09.018

Schneider, C. A., Rasband, W. S., & Eliceiri, K. (2012). NIH Image to ImageJ: 25 years of image analysis. *Nature Methods, 9,* 671−675.

Sobol, I. M. (1993). Sensitivity estimates for nonlinear mathematical models. *Mathematical Modelling and Computational Experiments, 1,* 407−414.

Toffin, E., Di Paolo, D., Campo, A., Detrain, C., & Deneubourg, J.-L. (2009). Shape transition during nest digging in ants. *Proceedings of the National Academy of Sciences of the United States of America, 106*(44), 18616−18620. https://doi.org/10.1073/PNAS.0902685106

van Beest, F. M., Mews, S., Elkenkamp, S., Schuhmann, P., Tsolak, D., Wobbe, T., Bartolino, V., Bastardie, F., Dietz, R., von Dorrien, C., Galatius, A., Karlsson, O., McConnell, B., Nabe-Nielsen, J., Olsen, M. T., Teilmann, J., & Langrock, R. (2019). Classifying grey seal behaviour in relation to environmental variability and commercial fishing activity − a multivariate hidden Markov model. *Scientific Reports, 9*(1), 1−14. https://doi.org/10.1038/s41598-019-42109-w

Van Rossum, G., & Drake, F. L. (2009). *Python 3 reference manual.* CreateSpace.

Varoudis, T., Swenson, A. G., Kirkton, S. D., & Waters, J. S. (2018). Exploring nest structures of acorn dwelling ants with X-ray microtomography and surface-based three-dimensional visibility graph analysis. *Philosophical Transactions of the Royal Society B: Biological Sciences, 373*(1753), Article 20170237. https://doi.org/10.1098/RSTB.2017.0237

Viterbi, A. J. (2006). A personal history of the Viterbi algorithm. *IEEE Signal Processing Magazine, 23*(4), 120−142.

White, J. W., Rassweiler, A., Samhouri, J. F., Stier, A. C., & White, C. (2014). Ecologists should not use statistical significance tests to interpret simulation model results. *Oikos, 123*(4), 385−388. https://doi.org/10.1111/J.1600-0706.2013.01073.X

Appendix

To check how stable agent-based model results are to a change in parameters, we conducted a sensitivity analysis using Sobol's method (Cariboni et al., 2007; Sobol, 1993). We used circular spread as the output variable.

Methods

The Sobol's method enables us to identify the contribution of variation in each model parameter to the total output variance, both on its own and in combination with other parameters. Briefly, the variance in the measured output, $V(Y)$, is decomposed as

$$V(Y) = V_1 + V_2 + \ldots + V_M + K \qquad (A1)$$

where V_i is the contribution of parameter i to the variance, M is the number of parameters and K is the residual. From this decomposition, it is possible to calculate the proportion of output variance contributed by each parameter without accounting for its interactions with other parameters, its first-order effect or S_i:

$$S_i = \frac{V_i}{V(Y)} \qquad (A2)$$

The output variance of a simulation model is estimated by running the model across parameter space, spanning the entire parameter distribution.

We used Saltelli's computational optimization of the Sobol's method (Saltelli, 2002; Saltelli et al., 2010), across the parameter space shown in Table A1. We used a sample size of 1000, which, through Saltelli's sampling method, generates 16 000 unique parameter combinations (Saltelli's sampling method starts from the given sample size to generate $Z = N \times (2M + 2)$ parameter combinations, where N is sample size and M the number of parameters). For each parameter combination, we ran the model once and measured distance and circular spread over the last 1000 time steps. Note that running a single simulation per combination causes some simulation noise to be incorporated into the parameter effect estimates. This is taken into account by looking at the confidence interval for the effect value. Simulations were run with 3000 stones and for a number of rounds $T = 5000$, as are the results for the 'intermediate stone availability' condition presented in the main text.

The SALib library was used for the analysis (run in Python 3.7.9).

Results and Discussion

The effect values calculated through the Sobol's method (Table A2) show that the only parameter with a relatively strong first-order effect (explaining 15% of the total variance) was G_m. To see how model results change in practice, we can take an in-detail look at how wall quality changes across parameter space, by examining the distribution of circular spread values (Fig. A1). The distribution shows that the revised model produces very consistent results. As a reminder (see Methods in the main article for details), the possible range of circular spread values goes from 0 (stones are perfectly evenly distributed in a circle, without gaps) to 1 (all stones are deposited in the same spot). These results indicate that the wall structure is clearly circular, with very few gaps, no matter what the model parameters are. Moreover, across the parameter space, the revised model tends to perform better than the original model (noticeable from a comparison with Fig. 3c; note that some of the simulations in Fig. 3c for the revised model and 3000 stones have slightly higher circular spread values, albeit still close to the zero end of the range − this is due to random variation).

Table A2
First-order effect and total effect of each parameter on circular spread

Parameter	S_i	S_i confidence interval
P_M	0.098	0.064
D_M	0.072	0.066
F_M	0.030	0.068
G_M	0.022	0.067
F_m	0.092	0.053
G_m	0.144	0.095
τ	0.030	0.075

First-order effects and total effects of model parameters as calculated with Sobol's variance decomposition. The 95% confidence interval was used.
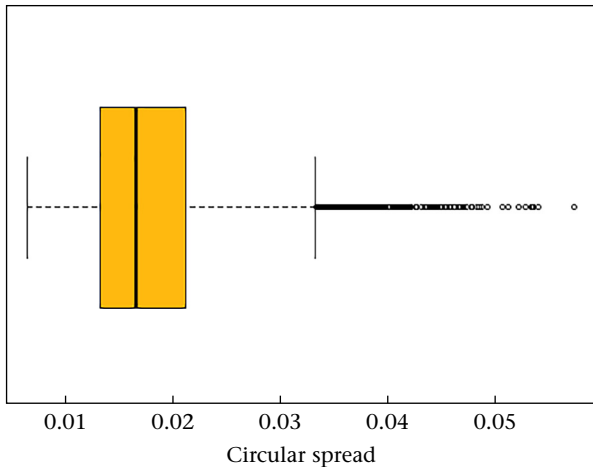
Table A1
Parameter range used for the sensitivity analysis

Parameter	Description	Boundaries
P_M	Maximum possible value of pick-up probability	[0.01,1]
D_M	Maximum possible value of deposition probability	[0.01,1]
F_M	Effect of number of stones on pick-up probability below a critical number of nearby stones S_c	[0.11,1]
G_M	Effect of number of stones on deposition probability above the critical number of nearby stones S_c	[0.11,1]
F_m	Effect of number of stones on pick-up probability above a critical number of nearby stones S_c	[0.001,0.1]
G_m	Effect of number of stones on deposition probability below a critical number of nearby stones S_c	[0.001,0.1]
τ	Parameter regulating the slope of the decrease in deposition probability and increase in pick-up probability as we move away from the optimal building distance	[0.01,0.03]

The table contains a summary description of the parameters used in the model with the range explored in the sensitivity analysis. Table from Invernizzi (2022).

Figure A1. Distribution of circular spread values across agent-based model parameter space. Edges of the plot indicate the edges of the lower and upper quartile. Whiskers indicate the edges of the bottom and top quantile. Outliers are shown.
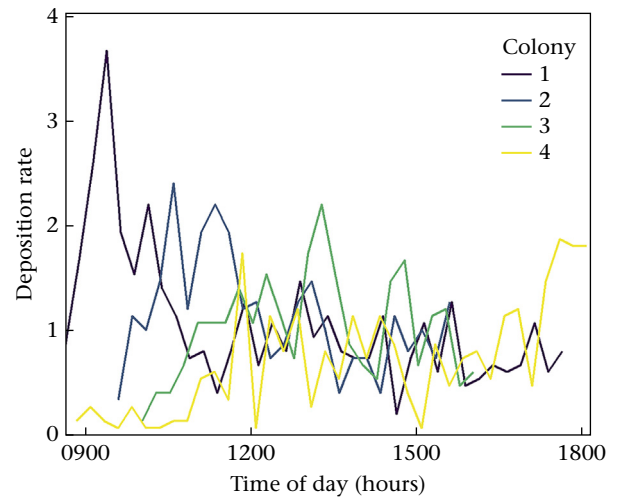

Figure A3. Deposition rate for each colony plotted against the corresponding time of day. The first time point for each time series corresponds to 15 min from the start of building activity, as in Fig. 4. All experiments started in the early morning and building activity started after a length of time lasting between 7 min and 2 h, during which the ants were initiating migration to the new nest.
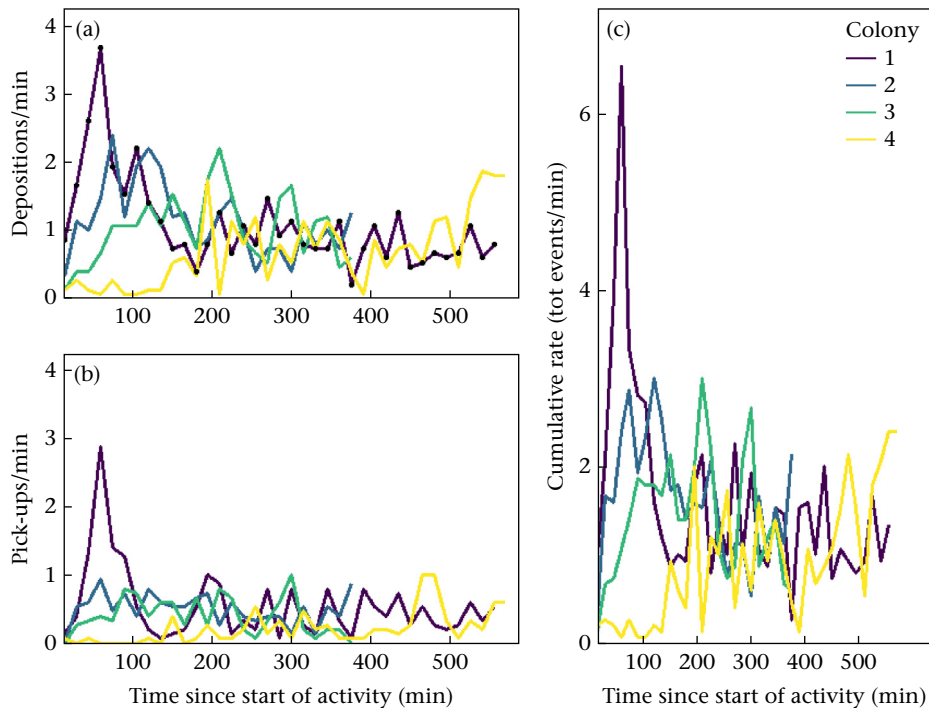

Figure A2. Activity rates of each colony from the start of building activity to the end of data collection: (a) deposition rate; (b) pick-up rate; (c) cumulative rate. Rates are at the colony level, calculated as the total number of events across the three sites, divided by the time interval. The cumulative rate was calculated as deposition rate + pick-up rate. The start of building was defined as the first deposition event in the colony and observation ended for a colony when at least 60 stones had been deposited at all three building sites under observation. Black dots in (a) correspond to individual time points (same for each time series). Each rate value was calculated over a 15 min interval. Values are plotted at the period's last minute time point; the first time point is therefore plotted at +15 min from the start of building and the rate value for that time point is calculated over minutes 0–14 of the observation period.
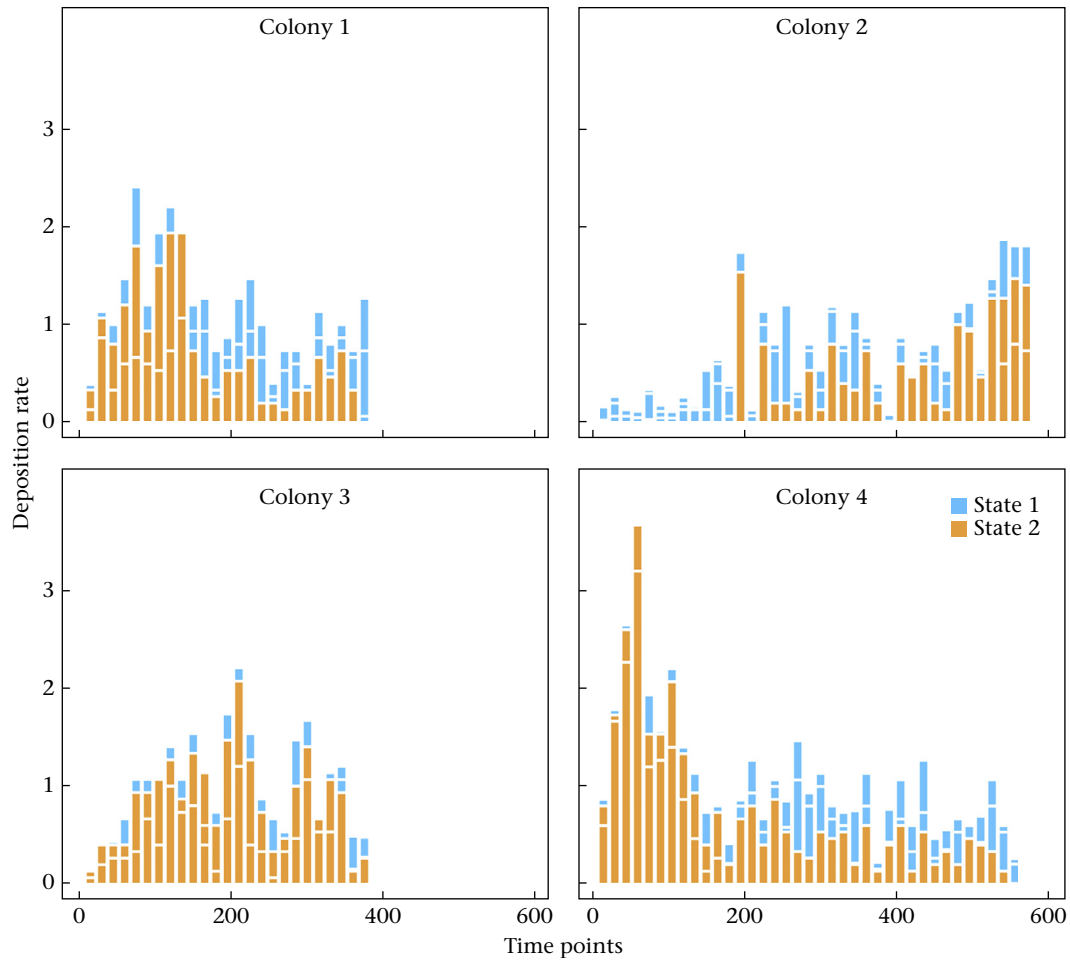
Figure A4. Change in deposition rate throughout building time for each colony, colour-coded by the estimated state sequence of each building site (stacked bars). The state sequence was estimated from the best model (deposition rate ~ stone density + (stone density)^2; Tables 2 and 3). The model assumes the existence of two behavioural states, high activity and low activity, generating distinct deposition rate probability distributions. Two sites within the same colony can be in different states at the same time point, as discussed in the main text. The two distributions are partially overlapping but clearly separate (Fig. 5), so that an observed sequence of higher rate values is likely to belong to a period of high activity (state 2) and a sequence containing both high and low values is likely to belong to a period of low activity (state 1). For time points with only two stacked bars visible, deposition rate was equal to zero at the third site.